Neutrophils are essential for induction of vaccine-like effects by antiviral monoclonal antibody immunotherapies

Mar Naranjo-Gomez, Jennifer Lambour, Marc Piechaczyk, Mireia Pelegrin

Neutrophils are essential for induction of vaccine-like effects by antiviral monoclonal antibody immunotherapies

Authors:

Mar Naranjo-Gomez, Jennifer Lambour, Marc Piechaczyk* and Mireia Pelegrin*

*Co-senior authors

Address:

"Equipe Labellisée par la Ligue contre le Cancer" - Institut de Génétique Moléculaire de Montpellier, University of Montpellier, CNRS, Montpellier, France

Lead contact:

Mireia Pelegrin
Institute of Molecular Genetics of Montpellier
1919, route de Mende
34293 Montpellier Cedex 5
France
mireia.pelegrin@igmm.cnrs.fr
Phone number: + 33 4 34 35 96 68
Fax number: + 33 4 34 35 96 34

KEY WORDS

Antiviral immunity, antiviral monoclonal antibodies, immunotherapy, B-cell helper neutrophils, vaccine-like effects.

ABSTRACT

Using a mouse retroviral model, we have shown that monoclonal antibody (mAb)-based immunotherapy can induce life-long endogenous protective immunity (vaccine-like effects). This observation has potentially important consequences for treating life-threatening human viral infections. Here, we investigated the role of neutrophils in this effect. Neutrophils are innate immunity effector cells with well-established microbe-killing activities that are rapidly mobilized upon infection. They are also emerging as orchestrators of innate and adaptive immunities. However, their immunomodulatory activity during antiviral mAb immunotherapies has never been studied. Our data reveal that neutrophils have an essential role in immunotherapy-induced immune protection of infected mice. Unexpectedly, neutrophils have a limited effect in controlling viral propagation upon passive immunotherapy administration, which is mostly mediated by natural killer cells (NKs). Instead, neutrophils operate as essential inducers of a potent host humoral antiviral response. Thus, neutrophils play an unexpected key role in protective immunity induction by antiviral mAbs. Our work opens new approaches to improve antiviral immunotherapies as they suggest that preserving neutrophil functions and counts might be required for achieving mAb-induced protective immunity.

INTRODUCTION

Neutralizing monoclonal antibodies (mAbs) are now considered as a potential therapeutic approach for the prevention and treatment of chronic and acute viral infections, including newly emerging viral infections (1). In recent years, there has been a dramatic increase in the development of new mAbs with improved neutralizing activity (1–14). Notably, in addition to anti-respiratory syncytial virus (RSV) mAb used to treat infant respiratory disease, several mAbs directed against human cytomegalovirus, human immunodeficiency- (HIV), influenza-, Ebola- and rabies virus are currently engaged in promising clinical trials (1, 3, 9, 14). While the direct effects of antiviral mAbs on viral propagation have been studied extensively, little attention has been paid to their potential immunomodulatory effects until recently (10, 15, 16).

Using a mouse model of persistent retroviral infection, the erythroleukemia induced by the Murine Leukemia Virus FrCasE, we have shown that treatment of infected mice with a highly neutralizing mAb can induce life-long protective immunity (vaccine-like effects) (see 10). This observation may have major therapeutic implications for humans. Indeed, increased antiviral immune responses after mAb treatments were recently observed in preclinical models of HIV, RSV and henipavirus infections (see 10). Moreover, passive immunotherapy with broadly neutralizing mAbs stimulated antiviral antibody responses in HIV-1-infected patients (14). Similarly, vaccine-like effects have also been documented in preclinical models of cancer immunotherapies (17–19), as well as in clinical trials using anti-CD20, anti-EGFR or anti-HER2 mAbs (20–23). Yet, neither the mechanisms at play nor the possible long-term protective consequences have been addressed in such clinical trials.

In humans, technical-, ethical- and cost limitations strongly limit investigations. Instead, immunocompetent animals offer the possibility to identify the cellular and molecular actors of antiviral mAb-induced vaccine-like effects. The FrCasE-induced erythroleukemia is a model system permitting extensive analysis of the endogenous immune response after passive mAb-based immunotherapy under conditions of both chronic infection and pathological development. We found that a 5-day treatment of FrCasE-infected mice with the neutralizing mAb 667 (an IgG2a recognizing the retroviral envelope glycoprotein; Env) shortly after infection provides long-lasting (> 1 year)

protective antiviral immunity of the Th1 type with enhanced IgG2a humoral- and cytotoxic T cell (CTL) responses and reduced regulatory T-cell activity (24–29). The immunomodulatory action of mAb 667 depends on its ability to interact with receptors for IgGs (FcγR). Notably, immune complexes (ICs) formed between the administered mAb and viral determinants enhance antiviral CTL responses through FcγR-mediated binding to dendritic cells (DCs) (27).

Importantly, IC-FcγR interactions concern several FcγR-bearing innate effector cells other than DCs, including neutrophils that are rapidly recruited at sites of infections. While they have long been viewed as simple and direct scavengers of extracellular pathogens, there is recent evidence that neutrophils can be key cells in the orchestration of innate and adaptive immunity via the interaction with different myeloid and lymphoid cells and the modulation of their functions (30, 31). However, their role in antiviral immunity is still largely unknown. Indeed, most investigations have studied neutrophil functions in viral pathogenesis or in the control of viral propagation through their effector functions, i.e. phagocytosis, reactive oxygen species production, neutrophil extracellular traps formation, etc. (32, 33). In contrast, the immunomodulatory properties of neutrophils have been poorly studied in viral infections and not addressed in the context of antiviral immunotherapies.

Here, we used the FrCasE model to address the general question of neutrophils participation in the induction of protective immunity by antiviral mAbs. We found that they are essential for the protection of infected, 667-treated mice. Unexpectedly, and unlike NKs, neutrophils had a limited effect on viral propagation control. Instead, their protective effect relied on their capacity to induce potent humoral responses due to the acquisition of B-cell-helper activity upon mAb treatment. Our findings should facilitate improved design of mAb-based antiviral therapies as they suggest that preserving neutrophil functions and counts might be required for achieving optimal protection by mAb.

RESULTS

Neutrophils are necessary for protection of infected mice by antiviral mAb without affecting viral propagation. We first addressed neutrophil mobilization in FrCasE-infected mice with, or without, 667 mAb treatment (infected/treated *vs* infected/non-treated). Passive immunotherapy was administered on the same day after establishment of viral infection (27) (Figure 1A, upper part) and at days 2 and 5 p.i. Age-matched naive mice were used as controls. Neutrophil recruitment was assessed in the spleen, one of the most viremic organs, at day 8 p.i, when viral replication is maximal in infected/non-treated mice (27). Neutrophil abundance in infected/treated mice was comparable to that observed in naive mice, whereas it was significantly higher in infected/non-treated animals (Figure 1B). Interestingly, this increased neutrophil frequency was associated with a higher percentage of spleen infected cells (Figure 1C), as assessed by flow cytometry using the H34 antibody (recognizing a Gag protein epitope expressed on the surface of FrCasE-infected cells) (34–36).

Next, we assessed the role of neutrophils in the control of viral propagation, as well as in the protection against leukemia in infected mice, with or without 667 mAb treatment. To this end, neutrophils were depleted by administering a mAb (1A8) directed to their specific Ly6G cell surface marker (37, 38) or an isotype control mAb (2A3). Depletion started 1 day before infection (Figure 1A, lower part), was efficient and specific (Supplemental Figure 1), and was maintained for 21 days, i.e. the time necessary to eliminate the therapeutic 667 mAb (27). Neutrophil elimination accelerated disease development in infected/non-treated mice and drastically reduced protection provided by 667 to infected mice (Figure 1D). We next assessed viral propagation in the different groups of mice. In infected/non-treated animals, neutrophil depletion (Figure 2A) was associated with a significant increase in the percentage of infected spleen cells at days 8 (Figure 1E) and 14 p.i. (Supplemental Figure 2A) as well as with a higher viremia (Supplemental Figure 2B). In contrast, in infected/treated mice, viral propagation was not significantly affected at days 8- (Figure 1E) and 14- p.i. (Figure 2B and Supplemental Figure 2) upon neutrophil depletion and remained lower than in infected/non-treated mice. This suggested that viral control by 667 mAb involved other innate immunity effector cells.

Thus, neutrophils exert different antiviral effects on FrCasE-infected mice depending on immunotherapy. In animals undergoing simple infection, neutrophils participate in the control of viral propagation. Instead, in infected/treated mice, they are crucial during the immunotherapy period for generation of long-term protection against leukemia, despite their limited effect on viral propagation.

NKs control viral propagation in infected/treated mice. As NKs can exert antibody-dependent cellular cytotoxicity (ADCC) activity against infected cells exposing determinants such as the retroviral Env protein (27, 39, 40), we asked whether NKs were involved in the control of viral propagation in infected/treated mice. To this end, NK cells were depleted using an anti-asialo-GM1 antibody (41–44) (Figure 2A). Contrasting to neutrophil depletion, the absence of NKs in infected/treated mice led to a significantly increased viral propagation at day 14 p.i. (Figure 2B). Next, we compared 667-mediated ADCC activity of NKs and neutrophils against infected cells using an in vivo antibody-mediated killing assay relying on the administration of 667-opsonized FrCasE-infected splenocytes in naive mice (27) (Figure 2C). Depletion of NKs, but not neutrophils, led to reduced mAb-mediated infected cell lysis (Figure 2D). Finally, as NKs are crucial for viral propagation control during the immunotherapy period, we assessed their role in the protection against leukemia in infected/treated mice. Importantly, NKs depletion drastically reduced survival of immunotreated mice (Figure 2E), indicating that antibody-mediated control of viral propagation by NKs is necessary for long-term antiviral protection.

Thus, NKs are crucial for protection of infected/treated mice via efficient control of viral propagation by 667-mediated ADCC.

Neutrophils differentially alter innate lymphoid cells biology in infected/treated- and infected/non-treated mice. Innate lymphoid cells (ILC) are a heterogeneous population of immune cells that includes NK cells and ILC1, ILC2 and ILC3. As NK biology can be affected by neutrophils (45), we first assessed the effect of neutrophil depletion on NKs. To this end, we measured the frequency of $CD3^{-}NKp46^{+}$ cells in the spleen of mice from the different groups. $CD3^{-}NKp46^{+}$ population mostly

identifies NKs but it may also include ILC1 and a subpopulation of ILC3 cells. NK cells can be distinguished from such ILCs using the cell surface marker CD49b (46). Notably, over 95 % of $CD3^-$ $NKp46^+$ cells were $CD49b^+$ (Supplemental Figure 3) indicating that the vast majority of $CD3^-NKp46^+$ cells in the spleen displayed a NK phenotype. As shown in Figure 3A, $CD3^-NKp46^+$ cells recruitment in spleens of both infected/non-treated and infected/treated mice at day 14 p.i. was similar and stronger than in naive mice. We also observed that neutrophils were involved in $CD3^-NKp46^+$ cells mobilization in infected/non-treated mice but neither in infected/treated- nor in naive mice (Figure 3A). We next assessed the frequency of splenic ILCs, other than NKs, by quantifying CD117 and CD127 expression in the $NKp46^+$ spleen cell population lacking the common lymphoid and myeloid lineage (Lin)-associated markers (Lin^-) (47). The recruitment of those ILCs in spleens of both infected/non-treated and infected/treated mice at day 14 p.i. was not significantly different from that observed in naive mice (Figure 3B). In addition, neutrophil depletion did not significantly alter the frequency of such ILCs (Figure 3B) in any group of mice.

These results show an enhanced recruitment of $CD3^-NKp46^+$ cells, which are mostly NK cells, in both infected/treated and infected/non-treated mice but these effects are neutrophil-dependent only in the latter. They also show that neutrophil depletion does not affect the frequency of splenic Lin^- $CD117^+CD127^+$ ILCs, in agreement with the lack of effect of anti-Ly6G-mediated-neutrophil depletion on splenic ILCs reported in other experimental settings (47).

To better characterize the effect of neutrophils on splenic $CD3^-NKp46^+$ cells, we assessed their maturation by monitoring CD11b and CD27 expression at day 14 p.i. These markers identify different stages of NK maturation in mice (45). Relative to naive mice, both infected/non-treated and infected/treated mice showed similar higher frequencies of $CD11b^+$ $CD3^-NKp46^+$ cells (including fully mature $CD11b^+CD27^-$- and semi-mature $CD11b^+CD27^+$- cells) (Figure 3C) at the expense of immature ones ($CD11b^-$) (not shown). Moreover, depletion of neutrophils entailed a strong reduction of the frequency of $CD11b^+$ $CD3^-NKp46^+$ cells only in infected/non-treated mice. Further characterization of $CD3^-NKp46^+$ cells indicated higher neutrophil-dependent IFN-γ production in infected/treated mice but low and similar IFN-γ levels in naive and infected/non-treated animals, whether the latter were

neutrophil proficient or deficient (Figure 3D). Finally, we assessed whether neutrophils affected the ADCC activity of NKs in infected/treated mice. Notably, ablation of neutrophils did not alter 667-mediated ADCC activity of NK cells (Figure 3E), consistent with the lack of effect on viral propagation (Figure 1E and 2B).

Thus, $CD3^-NKp46^+$ maturation is similarly enhanced in both infected/treated and infected/non-treated mice but these effects are neutrophil-dependent only in the latter. Nevertheless, neutrophils might participate in functional activation of $CD3^-NKp46^+$ cells in infected/treated animals, as our results show that neutrophils modulate their IFN-γ secretion capacity in infected/treated mice.

Neutrophils are crucial for inducing the humoral, but not the $CD8^+$ T-cell, antiviral response in immunotherapy-treated mice. Since neutrophils exert no control of viral propagation during the immunotherapy period (Figure 1E and 2B) but are necessary for long-term protection of mice (Figure 1D), we asked whether they could be key for the induction of vaccine-like effects.

We first addressed cellular adaptive immunity by assaying the primary virus-specific $CD8^+$ T-cell response in infected/non-treated and infected/treated mice at its peak (i.e. 14 days p.i.) (27) with or without neutrophils depletion. Consistent with our previous work, infected/treated mice showed an increased virus-specific $CD8^+$ T-cell response relative to infected/non-treated mice. In neither case the frequency of virus-specific $CD8^+$ T cells was altered by neutrophil depletion (Figure 4A). Similarly, neither case showed any difference in the frequency of $CD8^+$ T cells expressing IFN-γ (Figure 4B). These data ruled out a major role for neutrophils in the 667 mAb-induced anti-viral $CD8^+$ T-cell response.

Next, we addressed humoral immunity in infected/non-treated and infected/treated mice, depleted or not in neutrophils. To achieve this, anti-FrCasE serum immunoglobulins (Ig) from mice of the different groups were assayed by ELISA. Virus-specific IgM titers were assayed at 14 days p.i. (i.e. at the peak of the IgM response upon FrCasE infection and 667 treatment, Supplemental Figure 4) and were not significantly different between infected/non-treated and infected/treated mice (Figure 5A).

Interestingly, neutrophils depletion did not alter virus-specific IgM titers in either infected/non-treated or infected/treated mice (Figure 5A). In agreement with published studies in other experimental settings, the absence of neutrophils did not affect the levels of IgM (48). On the contrary, and consistent with our previous work (27), infected/treated mice displayed a much higher level of anti-FrCasE IgGs than infected/non-treated animals (Figure 5B), with a peak (700 µg/ml) by day 68 post-infection and a still high level (100 µg/ml) at the end of the experiment. Interestingly, in the absence of neutrophils, serum concentration of antiviral IgGs dramatically decreased in infected/treated mice (Figure 5B and Supplemental Figure 5). In contrast, neutrophils showed no role in the regulation of the poor non-protective antibody response elicited in infected/non-treated mice (Figure 5B). Importantly, high anti-FrCasE IgG seric levels correlated with longer survival times, supporting a role for the high humoral antiviral response in protection against disease (Figure 5C). To further characterize the long-term virus-specific humoral response, we tested whether infected/treated mice, depleted or not in neutrophils, could respond to a virus challenge performed 3 months after the first infection (i.e. a time point at which the primary humoral response has strongly declined). Infected/treated mice, depleted or not in neutrophils, were inoculated with FrCasE and serum samples were collected 1 week later to assay the generation of endogenous anti-FrCasE antibodies. In the presence of neutrophils, 3 out of 5 infected/treated mice showed an increase in the virus-specific humoral response (Figure 5 D) while, in the absence of neutrophils, none of the infected/treated mice responded to the viral challenge. Altogether, these results show that neutrophil depletion at early time points after infection and treatment affects humoral immunity with an effect on both primary and memory virus-specific B-cell responses.

As marginal zone (MZ) B cells are known to contribute to the mounting of antibody responses (49, 50) and their function might be modulated by neutrophils (51), we next addressed the frequencies of splenic MZ (CD21highIgMhigh CD19+ cells)- and follicular (FO) (CD23+IgMlow CD19+ cells) B cells. MZ B-cells frequency was enhanced in a neutrophil-dependent manner in infected/treated mice but unchanged in infected/non-treated animals relative to naive mice (Figure 6A). In contrast, the frequency of FO B cells was significantly enhanced in infected/treated mice relative to naive mice,

with however no role for neutrophils (Figure 6B). Interestingly, consistent with a role of MZ B cells in the generation of plasma cells (49), the higher frequency of splenic MZ B cells at day 14 p.i. in infected/treated mice was associated with a higher frequency of $CD138^+$ plasma cells in bone-marrow (BM), as compared to infected/non-treated animals. This effect was neutrophil-dependent (Figure 6C). Finally, histological analyses of spleens of infected mice at 14 days p.i. revealed larger germinal centers (GC, defined by staining of MZ $CD169^+$ macrophages and $B220^+$ cells) in infected/treated versus infected/non-treated mice (Figure 6D). In agreement with a role of neutrophils in the enhancement of the humoral response, neutrophil depletion in infected/treated mice led to smaller GCs (Figure 6D).

Thus, neutrophils are essential for the vaccine-like effects induced by the 667 immunotherapy through the stimulation of the humoral, but not the $CD8^+$ T-cell, antiviral response. This effect is associated with a neutrophil-dependent increase in both splenic MZ B cells and BM plasma cells.

Neutrophils are differently activated in infected/-treated- and -non-treated mice. Finally, we addressed the functional activation of splenic neutrophils in infected mice with or without 667 immmunotherapy at day 8 p.i. by monitoring cell surface activation markers and quantifying various cytokine mRNA and protein levels. In infected/treated- and infected/non-treated mice, splenic neutrophils were similarly activated, as deduced from CD62L shedding and increased expression of CD11b (Figure 7A). However, neutrophils from infected/treated mice showed a significantly stronger expression of two cytokines involved in B-cell activation, B cell-activating factor (BAFF) and lymphotoxin α (LTα), compared to infected/non-treated animals (Figure 7B), suggesting a role for the therapeutic mAb in the functional activation of neutrophils. Splenic neutrophils sorted from infected/treated mice also showed a trend for higher secretion capacity of BAFF and LTα, as compared to infected/non-treated mice neutrophils, even though such a trend did not reach statistical significance. To further assess whether mAb-triggering (through FcγR cross-linking) could enhance BAFF and LTα release by neutrophils, we isolated BM neutrophils from naive mice and stimulated them for 24 h in plates coated with the 667 mAb. Experiments were conducted in the presence or the absence of the pro-

inflammatory cytokine IFN-γ to assess the extent to which inflammatory conditions could synergize with 667 mAb-triggering. Interestingly, in the presence of IFN-γ, 667 mAb triggering led to a significantly increased release of BAFF and LTα by neutrophils (Figure 7C).

In summary, FrCasE infection activates neutrophils independently of immunotherapy. However, the activation state significantly differs between the two groups of animals, notably with a significantly stronger expression of LTα and BAFF in immunotherapy-treated mice. In addition, inflammatory conditions synergize with mAb-mediated activation of neutrophils leading to an enhanced release of BAFF and LTα.

DISCUSSION

We have previously shown that antiviral mAb-based therapies can induce life-long protective immunity. This finding potentially has important therapeutic implications, as evidence suggests that it may also apply to diverse severe human viral diseases (10, 14). A paramount task is now to identify the mechanisms at the origin of the mAb-induced vaccine-like effects and exploit them for more efficient mAb-based treatment of patients.

Here, we report that neutrophils are essential during the immunotherapy period for long-term survival of FrCasE-infected mice, not because they control viral propagation but because they are crucial for inducing a protective humoral response without an effect on the $CD8^+$ T-cell response. In contrast, we show that, upon 667 mAb treatment, NKs are crucial for the elimination of infected cells by 667-mediated ADCC activity and are necessary for long-term survival of infected/treated mice. Thus, our work indicates that both innate effector cells have distinct but complementary roles in the protection of infected mice by mAb; NKs have an early and predominant role in the control of viral spread while neutrophils are essential for the emergence of a potent host antiviral humoral response. Our findings contrast with the current view of neutrophils usually considered as simple frontline agents against invading pathogens and highlight the hitherto unreported role of neutrophils as key cells in the modulation of adaptive antiviral immunity upon mAb treatment**.**

Our data indicate that survival of infected/treated mice depends on an efficient anti-FrCasE humoral response. Infected/treated mice show neutrophil-dependent (i) increased frequency of MZ B cells, (ii) enhanced formation of GCs, (iii) increased plasma cell generation and (iv) enhanced production of antiviral IgGs. Interestingly, the absence of neutrophils during the immunotherapy period in infected mice also leads to impaired development of secondary humoral responses upon viral challenge. Overall our data suggest that neutrophils are essential for antiviral protection due to their B-cell-helper activity. Similarly, such a helper function has already been documented under homeostatic conditions (51), in autoimmunity disease-prone mice (52), during emergency granulopoiesis (53) and in bacterial infection (54). Importantly, our findings show that the acquisition of B-cell helper functions in

295 infected mice is dependent on immunotherapy, as no modulation of the anti-FrCasE humoral response
296 was detected in infected/non-treated mice upon neutrophil depletion.

297 Though not excluding the role of other factors, our study suggests potential roles for BAFF and LTα
298 in this B-cell helper function. As concerns BAFF, it is interesting to note that its secretion by splenic
299 neutrophils can contribute to the activation of splenic MZ B cells and the acceleration of plasma cell
300 generation (51, 55). Moreover, BAFF administration to mice increases both the frequency of MZ B
301 cells and antibody production (56, 57) and constitutes a signal for both MZ B cell survival and
302 differentiation into plasmablasts (47, 58–61) . Together with the fact that MZ B cells can favor the
303 generation of plasma cells upon microbial infection (49), it is reasonable to speculate that BAFF
304 induction in neutrophils of infected/treated mice may also favor the MZ B cell response and the
305 subsequent generation of plasma cells. Interestingly, in agreement with our in vitro results showing
306 enhanced BAFF release by neutrophils upon combination of IFN-γ stimulation and FcγR cross-link
307 (Figure 7C), different pro-inflammatory stimuli, including ICs, have been shown to act as
308 secretagogues and to synergize with IFN-γ to enhance BAFF secretion by human neutrophils (62).
309 Moreover, neutrophil depletion in autoimmunity-prone mice led to a reduction of auto-antibodies titers
310 that correlated with decreased serum levels of IFN-γ and BAFF (52). Thus, it can reasonably be
311 hypothesized that inflammatory conditions synergize with ICs formed after 667 mAb-treatment of
312 FrCasE-infected mice to enhance BAFF release by neutrophils.

313 Although not formally shown, our data suggest that LTα release by neutrophils might play a role in
314 the enhancement of the antiviral humoral response in infected/treated mice. LTα is involved in the
315 formation of secondary lymphoid organs, it is expressed by lymphocytes and mediates a large variety
316 of inflammatory and antiviral responses. It has also been reported to play a role in the development of
317 GC formation and to be required for IgG responses (63–65). Here, we show that this cytokine is
318 expressed and released by neutrophils upon mAb treatment of infected mice. Interestingly, although
319 LTα is not known to be expressed by neutrophils, it has been proposed that non-lymphocytic murine
320 splenic cells are able to produce it (66). We also report that FcγR cross-linking by immobilized 667

mAb synergizes with IFN-γ to enhance LTα release by neutrophils. This suggests that, similarly to BAFF, inflammatory conditions and mAb-triggering might lead to increased LTα secretion by neutrophils. Further studies will be required to address whether BAFF and LTα combine their actions to stimulate the antiviral humoral response upon mAb immunotherapy. Finally, as IFN-γ potentiates both BAFF and LTα release, it will also be important to assess whether and how neutrophil-dependent IFN-γ production by NKs in infected/treated mice contributes to the stimulation of antibody responses, as this cytokine affects class-switching and long-term maintenance of neutralizing antibody titers in retrovirally-infected mice (34) and humoral autoimmunity in humans (67).

Identifying neutrophils as key players in the induction of protective immunity by antiviral mAbs has important therapeutic implications for several reasons. First, if combination therapies are considered, it will be of utmost importance that the agent(s) co-administered with the passive immunotherapy do not alter neutrophil functions and counts to avoid inhibiting efficient antiviral humoral immune responses. Second, in pathological situations leading to neutropenia and/or impaired neutrophils functions, such as certain viral infections (68, 69) and/or drug-induced neutropenia (70), it will be essential to restore them. This could, for example, be achieved through administration of granulocyte colony-stimulating factor (G-CSF) a cytokine already used in the clinic to treat neutropenic patients. Interestingly, this cytokine might also be used in combination with treatments aiming at enhancing the generation of functional neutrophils (70). Furthermore, beyond stimulating neutrophil activation and/or mobilization, G-CSF enhances neutrophil BAFF-secretion capacity and thereby their ability to stimulate B cells (71). Similarly, reduction of viral load by antiretroviral therapies also permits partial restoration of the impaired functions of neutrophils observed in HIV-infected patients (68). Interestingly, neutrophils have been shown to mediate immunosuppression via the PD-L1/PD-1 pathway in HIV-infected patients (72). Antiviral passive immunotherapies might therefore benefit from combination with the administration of mAbs targeting this immune checkpoint. Finally, alternative approaches, such as engineering the Fc fragment of antiviral mAbs, merit consideration. Increasing their affinity for the FcγRs expressed by neutrophils might, at first, allow superior antibody-mediated phagocytosis, as recently reported in the case the Fc-modified VR01 anti-HIV mAb (73).

348 This could then alter cell signaling and cytokine/chemokines production to ultimately lead to more
349 effective adaptive immune responses. Thus, stimulating neutrophil activity, restoring their impaired
350 functions and/or counteracting their immunosuppressive actions should improve the vaccine-like
351 effects of antiviral mAb-based immunotherapies. This might also apply to cancer treatment as
352 enhancement of antitumoral immune responses has also been observed in mAb-based anticancer
353 immunotherapies. This is all the more important to take into consideration as neutrophils have been
354 shown to play a role in the therapeutic activity of anticancer mAb (74–78).

355

METHODS

Ethical statement. Mice were bred and maintained under conventional, pathogen-free facilities at the Institut de Génétique Moléculaire de Montpellier. All experimental procedures were performed in accordance with the French national animal care guidelines (CEEA-LR-12146 approval).

Viral stocks. FrCasE viral stocks were produced, assayed and stored as described previously (27).

Viral infection, immunotherapy and mice follow-up. Eight day-old 129/Sv/Ev mice were infected intraperitoneally (i.p.) with 50 µl of a virus suspension containing 50,000 ffu (focus-forming units) and treated, or not, with 30 µg of 667 mAb 1 hour post-infection (p.i.) and on days 2 and 5 p.i. by i.p. administration. Mice were examined at regular intervals for clinical signs of erythroleukemia (reduction of hematocrits). They were euthanized when their hematocrits reached 35% (experimental endpoint).

Flow cytometry. Spleen single-cell suspensions were obtained by mechanical dissociation of the organs in PBS. Bone marrow (BM) cell suspensions were obtained by dissection and PBS-flushing of tibias and femurs. Cells were stained at 4°C using fluorochrome-conjugated antibodies to: CD3e (145-2C11), CD4 (RM4-5), CD8 (Ly2, 53-6.7), CD11b (M1/70), CD11c (HL3), CD19 (1D3), CD21/35 (eBio8d9), CD23 (B3B4), CD27 (LG3A10), CD45.2 (104), CD45R/B220 (RA3-6B2), CD49b (DX5), CD62L (Ly22, MEL-14), CD117 (2B8), CD127 (SB/199), CD138 (281-2), F4/80 (BM8), Gr1 (RB6-8C5), IFN-γ (XMG1.2), IgM (eB121-15F9), Ly6G (1A8), lineage (Ter119; Gr1; CD45R/B220; CD11c; F4/80; CD3e), NKp46 (29A1.4) (BD Bioscience, eBioscience or BioLegend). FrCasE-infected cells were assayed using an anti-Gag mAb (H34) (35) labelled with Alexa Fluor 647. Forward scatter area and forward scatter time-of-flight, as well as side scatter, were used to remove doublets from flow cytometry analyses. Cells were analyzed on FACSCanto II flow cytometer (BD Bioscience) and the data were analyzed using the FlowJo software (Tree Star).

383 *ELISA of anti-FrCasE antibodies.* Plasma anti-FrCasE immunoglobulins were assayed by ELISA as
384 already described (26, 27). Peroxidase-conjugated anti-mouse IgG or IgM rabbit antisera (Serotec)
385 were used as secondary antibodies.

386 *Virus challenge experiments***.** Infected/treated mice, depleted or not in neutrophils, were injected i.v.
387 with 300 µl of a 5 x 10^4 FFU/ml FrCasE suspension mixed to 2 x 10^6 FrCasE-infected splenocytes 3
388 months after the first infection. Blood samples were collected 1 week post-challenge to assay
389 endogenous anti-FrCasE IgG concentrations by ELISA.

390 *In vivo depletion of Ly6G$^+$ and NK cells.* Neutrophils were depleted by administering a rat anti-Ly6G
391 antibody (1A8; BioXcell), (37, 38) injected i.p. at different time-points (150 µg/injection) or isotype
392 control rat IgG (2A3; BioXcell). Neutrophils depletion was monitored by flow cytometry analysis of
393 Gr1^{high} and CD11b$^+$ cells. NKs were depleted using the anti-asialo GM1 antibody (Wako Pure
394 Chemical Industries, Ltd), injected i.p. at different time-points (50 µl/injection). This antibody has
395 been used to study the in vivo functions of NKs in mouse strains lacking the NK1.1 allotype, which is
396 a feature of 129 Sv/Ev mice (42).
397
398 *In vivo cytolysis activity*. Experiments were conducted as described in (27, 79). Briefly, red blood cell-
399 free splenocytes were recovered from 10 day-old FrCasE-infected-, or non-infected, pups. Splenocytes
400 from non-infected mice were labelled with the vital dye carboxy-fluorescein succinimidyl ester
401 (CFSE; Molecular Probes) at a concentration of 0.5 µM (CFSE^{low} cells). Splenocytes from infected
402 mice were labelled with 5 µM CFSE (CFSE^{high} cells) and pre-incubated, or not, with the 667 mAb (the
403 absence of 667 allows to quantify spontaneous cell death). Both cell populations were mixed at a 1:1
404 ratio before retrorbital administration to recipient mice. Cytolysis activity against infected splenocytes
405 was calculated from the ratio of CFSE^{low}/CFSE^{high} cells in spleen assayed by flow cytometry 5 hours
406 later. To assess the contribution of NKs and neutrophils to antibody-mediated cytolysis, 50 µl of the
407 anti-asialo GM1 or 200 µg of the anti-Ly6G 1A8 mAb were administered 1 day prior to the assay.
408

409 *Flow cytometry assay of CD8$^+$ T cells specific for FrCasE-infected cells*. Splenocytes were labelled
410 with both an APC-conjugated anti-CD8$^+$ T cell antibody and a PE-conjugated MHC class I H-2D^b
411 tetramer (Beckman Coulter) displaying the immunodominant Friend virus GagL epitope (27) (80) (D^b-
412 GagL tetramers) as previously described (27).
413
414 *Assay of IFN-γ production*. 10^6 splenocytes were incubated at 37°C for 5 hours in 12-well plates in
415 500 µl of RPMI culture medium containing phorbol 12-myristate 13-acetate (50 ng/ml) and ionomycin
416 (500 ng/ml) in the presence of brefeldin A (10 µg/ml; Sigma-Aldrich). IFN-γ production was flow
417 cytometry-assayed using the intracellular Cytofix/Cytoperm Fixation/Permeabilization staining kit
418 (Becton Dickinson).
419
420 *Histological analyses.* Spleens from infected/non-treated- and infected/treated mice (depleted or not in
421 neutrophils) were recovered at day 14 p.i. and prepared as previously described (81). Briefly, spleens
422 were initially fixed at 4°C overnight with a PLP (Paraformaldehyde-lysine-periodate) solution and
423 then embedded in 4% low temperature-gelling agarose (type VII-1; Sigma-Aldrich) prepared in PBS
424 (Phosphate Buffered Saline). 300 µm slices were cut with a vibratome (VT 1000S; Leica) in a bath of
425 ice-cold PBS. Sections of tissues were submerged in PBS and transferred to 0.4 µm organotypic
426 culture inserts (Millicell; Millipore) for staining with an anti-B220 (RA3-6B2, Becton Dickinson) and
427 an anti-CD169 antibody (MOMA-1, Biorad) at 37°C for 20 minutes. The images were captured using
428 a Leica SP8-UV confocal scanning microscope.
429
430 *RT-qPCR quantification of gene expression*. Single-cell suspensions of splenocytes were prepared
431 from naive, infected/non-treated and infected/treated mice 8 days p.i. and immunotherapy. Neutrophils
432 (CD11b$^+$Ly6G^{high} expression) were sorted (>98% pure) using a BD Biosciences FACSAria device.
433 RNA was extracted from 1-2 x 10^6 sorted neutrophils using the RNeasy micro kit (Qiagen). RNA
434 quality and integrity were verified using the Agilent 2100 bioanalyzer. cDNAs were synthesized using
435 the RT2 First Strand Kit (Qiagen). All quantitative PCRs were performed following protocols
436 optimized for the RT2 quantitative Profiler PCR array using SYBR Green mix (Qiagen) and

LightCycler 480 II machine (Roche). All data were normalized to β-actin. Results were expressed as fold increases with respect to naive cells using the ΔΔCt method.

BAFF and LTα protein release quantification. Soluble BAFF and LTα from cell-free supernatants of cultured neutrophils were assayed using BAFF (R&D Systems) and LTα ELISA (NeoBiotech), respectively. Supernatants were collected from sorted splenic neutrophils (from naive, infected/non-treated and infected/treated mice at 8 days p.i. and immunotherapy) cultured in 96-well plates at a density of $2x10^5$ cells/well for 24 h. Alternatively, neutrophils were isolated from naive mice BM using a magnetic-based cell-sorting (MACS) neutrophil isolation kit (>95% purity; Miltenyi Biotec) and cultured for 24 h in 667mAb-coated 24-well plates at a density of 2×10^6 cells in 500 µl of medium, in the presence or in the absence of IFN-γ (100 µg/mL). 667 mAb-non coated plates were used as controls. G-CSF (R&D Systems) was added at a concentration of 10 ng/ml to neutrophil cultures to maintain cell viability

Statistical analyses. Statistical analyses were performed using GraphPad Prism 5 (GraphPad Software). Data were expressed as means +/- SEM and statistical significance was established using a parametric one-way ANOVA test with a Bonferroni correction for multiple comparisons or unpaired Student's t tests when two groups were compared. p values lower than 0.05 were considered as statistically significant.

AUTHOR CONTRIBUTIONS

Mireia Pelegrin (MPe), MN-G and Marc Piechaczyk (MPi) defined the research program. MN-G, JL and MPe performed the experiments and carried out the data analyses with a contribution by MPi. MPe, MN-G and MPi wrote the manuscript. Grants to MPe and MPi funded the study.

ACKNOWLEDGEMENTS

This work was supported by grants from the Ligue Nationale Contre le Cancer, the Fondation ARC, Sidaction and the Fondation pour la Recherche Médicale. M. Naranjo-Gomez, J. Lambour, M. Piechaczyk and M. Pelegrin are members of the "MabImprove Labex", a public grant overseen by the French National Research Agency (ANR) as part of the "Investments for the future" program (reference: ANR-10-LABX -53-01) that also supported this work. We thank the imaging facility MRI, which is part of the UMS BioCampus Montpellier and a member of the national infrastructure France-BioImaging, supported by the French National Research Agency (ANR-10-INBS-04, "Investments for the future"). We are grateful to the animal facility of the Institut de Génétique Moléculaire de Montpellier which is part of the "Réseau des Animaleries Montpelliéraines" RAMIBiSA Facility for animal experiments and to the "Réseau d'Histologie Experimentale de Montpellier" RHEM Facility for expert assistance with histology. We are grateful to E. Donnadieu (Institut Cochin, Paris) for expert assistance with histology, to M. Boyer and S. Gailhac from MRI for support in cytometry experiments, to Thierry Gostan (SERENAD Complex Biological Data Analysis Service) for support in statistical analyses, to Helen Phillips Bevis (Traductions Stratégiques) for English editing services and to Drs. V. Dardalhon, M. Hahne and B. Hipskind for critical reading of the manuscript.

CONFLICT OF INTEREST DISCLOSURES

The authors declare no competing financial interests.

REFERENCES

1. Salazar G., Zhang, N., Fu, T.-M. Antibody therapies for the prevention and treatment of viral infections. *NPJ Vaccines 2017 Jul 10219*

2. Both L et al. Monoclonal antibodies for prophylactic and therapeutic use against viral infections. *Vaccine* 2013;31(12):1553–1559.

3. Caskey M et al. Antibody 10-1074 suppresses viremia in HIV-1-infected individuals. *Nat. Med.* 2017;23(2):185–191.

4. Corti D, Lanzavecchia A. Broadly neutralizing antiviral antibodies. *Annu. Rev. Immunol.* 2013;31:705–742.

5. Corti D et al. Prophylactic and postexposure efficacy of a potent human monoclonal antibody against MERS coronavirus. *Proc. Natl. Acad. Sci. U. S. A.* 2015;112(33):10473–10478.

6. Corti D et al. Protective monotherapy against lethal Ebola virus infection by a potently neutralizing antibody. *Science* 2016;351(6279):1339–1342.

7. De Benedictis P et al. Development of broad-spectrum human monoclonal antibodies for rabies post-exposure prophylaxis. *EMBO Mol. Med.* 2016;8(4):407–421.

8. Fibriansah G et al. A potent anti-dengue human antibody preferentially recognizes the conformation of E protein monomers assembled on the virus surface. *EMBO Mol. Med.* 2014;6(3):358–371.

9. Lynch RM et al. Virologic effects of broadly neutralizing antibody VRC01 administration during chronic HIV-1 infection. *Sci. Transl. Med.* 2015;7(319):319ra206.

10. Pelegrin M, Naranjo-Gomez M, Piechaczyk M. Antiviral Monoclonal Antibodies: Can They Be More Than Simple Neutralizing Agents? *Trends Microbiol.* 2015;23(10):653–665.

11. Bangaru S et al. Recognition of influenza H3N2 variant virus by human neutralizing antibodies. *JCI Insight* 2016;1(10). doi:10.1172/jci.insight.86673

12. Bailey JR et al. Broadly neutralizing antibodies with few somatic mutations and hepatitis C virus clearance. *JCI Insight* 2017;2(9). doi:10.1172/jci.insight.92872

13. Kam Y-W et al. Cross-reactive dengue human monoclonal antibody prevents severe pathologies and death from Zika virus infections. *JCI Insight* 2017;2(8). doi:10.1172/jci.insight.92428

14. Schoofs T et al. HIV-1 therapy with monoclonal antibody 3BNC117 elicits host immune responses against HIV-1. *Science* 2016;352(6288):997–1001.

15. Lambour J, Naranjo-Gomez M, Piechaczyk M, Pelegrin M. Converting monoclonal antibody-based immunotherapies from passive to active: bringing immune complexes into play. *Emerg. Microbes Infect.* 2016;5(8):e92.

16. Wen Y-M, Mu L, Shi Y. Immunoregulatory functions of immune complexes in vaccine and therapy. *EMBO Mol. Med.* 2016;8(10):1120–1133.

17. Abès R, Gélizé E, Fridman WH, Teillaud J-L. Long-lasting antitumor protection by anti-CD20 antibody through cellular immune response. *Blood* 2010;116(6):926–934.

18. Deligne C, Metidji A, Fridman W-H, Teillaud J-L. Anti-CD20 therapy induces a memory Th1 response through the IFN-γ/IL-12 axis and prevents protumor regulatory T-cell expansion in mice. *Leukemia* 2015;29(4):947–957.

19. DiLillo DJ, Ravetch JV. Differential Fc-Receptor Engagement Drives an Anti-tumor Vaccinal Effect. *Cell* 2015;161(5):1035–1045.

20. Hilchey SP et al. Rituximab immunotherapy results in the induction of a lymphoma idiotype-specific T-cell response in patients with follicular lymphoma: support for a "vaccinal effect" of rituximab. *Blood* 2009;113(16):3809–3812.

21. Srivastava RM et al. Cetuximab-activated natural killer and dendritic cells collaborate to trigger tumor antigen-specific T-cell immunity in head and neck cancer patients. *Clin. Cancer Res.* 2013;19(7):1858–1872.

22. Taylor C et al. Augmented HER-2 specific immunity during treatment with trastuzumab and chemotherapy. *Clin. Cancer Res.* 2007;13(17):5133–5143.

23. Trivedi S et al. Anti-EGFR Targeted Monoclonal Antibody Isotype Influences Antitumor Cellular Immunity in Head and Neck Cancer Patients. *Clin. Cancer Res.* 2016;22(21):5229–5237.

24. Gros L et al. Induction of long-term protective antiviral endogenous immune response by short neutralizing monoclonal antibody treatment. *J. Virol.* 2005;79(10):6272–6280.

25. Gros L, Pelegrin M, Plays M, Piechaczyk M. Efficient mother-to-child transfer of antiretroviral immunity in the context of preclinical monoclonal antibody-based immunotherapy. *J. Virol.* 2006;80(20):10191–10200.

26. Gros L et al. Endogenous cytotoxic T-cell response contributes to the long-term antiretroviral protection induced by a short period of antibody-based immunotherapy of neonatally infected mice. *J. Virol.* 2008;82(3):1339–1349.

27. Michaud H-A et al. A crucial role for infected-cell/antibody immune complexes in the enhancement of endogenous antiviral immunity by short passive immunotherapy. *PLoS Pathog.* 2010;6(6):e1000948.

28. Nasser R et al. Long-lasting protective antiviral immunity induced by passive immunotherapies requires both neutralizing and effector functions of the administered monoclonal antibody. *J. Virol.* 2010;84(19):10169–10181.

29. Nasser R, Pelegrin M, Plays M, Gros L, Piechaczyk M. Control of regulatory T cells is necessary for vaccine-like effects of antiviral immunotherapy by monoclonal antibodies. *Blood* 2013;121(7):1102–1111.

30. Mócsai A. Diverse novel functions of neutrophils in immunity, inflammation, and beyond. *J. Exp. Med.* 2013;210(7):1283–1299.

31. Scapini P, Cassatella MA. Social networking of human neutrophils within the immune system. *Blood* 2014;124(5):710–719.

32. Galani IE, Andreakos E. Neutrophils in viral infections: Current concepts and caveats. *J. Leukoc. Biol.* 2015;98(4):557–564.

33. Saitoh T et al. Neutrophil extracellular traps mediate a host defense response to human immunodeficiency virus-1. *Cell Host Microbe* 2012;12(1):109–116.

34. Stromnes IM et al. Temporal effects of gamma interferon deficiency on the course of Friend retrovirus infection in mice. *J. Virol.* 2002;76(5):2225–2232.

35. Chesebro B. Characterization of mouse monoclonal antibodies specific for Friend murine leukemia virus-induced erythroleukemia cells: friend-specific and FMR-specific antigens.. *Virol. 1981 Jul 151121131-44*

566 36. Dittmer U et al. Essential roles for CD8+ T cells and gamma interferon in protection of mice
567 against retrovirus-induced immunosuppression. *J. Virol.* 2002;76(1):450–454.

568 37. Carr KD et al. Specific depletion reveals a novel role for neutrophil-mediated protection in the
569 liver during Listeria monocytogenes infection. *Eur. J. Immunol.* 2011;41(9):2666–2676.

570 38. Daley JM, Thomay AA, Connolly MD, Reichner JS, Albina JE. Use of Ly6G-specific monoclonal
571 antibody to deplete neutrophils in mice. *J. Leukoc. Biol.* 2008;83(1):64–70.

572 39. Bruel T et al. Elimination of HIV-1-infected cells by broadly neutralizing antibodies. *Nat.*
573 *Commun.* 2016;7:10844.

574 40. Smalls-Mantey A, Connors M, Sattentau QJ. Comparative efficiency of HIV-1-infected T cell
575 killing by NK cells, monocytes and neutrophils. *PloS One* 2013;8(9):e74858.

576 41. Bodhankar S, Woolard MD, Sun X, Simecka JW. NK cells interfere with the generation of
577 resistance against mycoplasma respiratory infection following nasal-pulmonary immunization. *J.*
578 *Immunol.* 2009;183(4):2622–2631.

579 42. Carlyle JR et al. Molecular and genetic basis for strain-dependent NK1.1 alloreactivity of mouse
580 NK cells. *J. Immunol.* 2006;176(12):7511–7524.

581 43. Kasai M, Iwamori M, Nagai Y, Okumura K, Tada T. A glycolipid on the surface of mouse natural
582 killer cells. *Eur. J. Immunol.* 1980;10(3):175–180.

583 44. Ong S et al. Natural killer cells limit cardiac inflammation and fibrosis by halting eosinophil
584 infiltration. *Am. J. Pathol.* 2015;185(3):847–861.

585 45. Jaeger BN et al. Neutrophil depletion impairs natural killer cell maturation, function, and
586 homeostasis. *J. Exp. Med.* 2012;209(3):565–580.

587 46. Cortez VS, Robinette ML, Colonna M. Innate lymphoid cells: new insights into function and
588 development. *Curr. Opin. Immunol.* 2015;32:71–77.

589 47. Magri G et al. Innate lymphoid cells integrate stromal and immune signals to enhance antibody
590 production by splenic marginal zone B cells. *Nat. Immunol.* 2014;15(4):354–364.

591 48. Cerutti A, Cols M, Puga I. Marginal zone B cells: virtues of innate-like antibody-producing
592 lymphocytes. *Nat. Rev. Immunol.* 2013;13(2):118–132.

593 49. Song H, Cerny J. Functional heterogeneity of marginal zone B cells revealed by their ability to
594 generate both early antibody-forming cells and germinal centers with hypermutation and memory in
595 response to a T-dependent antigen. *J. Exp. Med.* 2003;198(12):1923–1935.

596 50. Zouali M, Richard Y. Marginal zone B-cells, a gatekeeper of innate immunity. *Front. Immunol.*
597 2011;2:63.

598 51. Puga I et al. B cell-helper neutrophils stimulate the diversification and production of
599 immunoglobulin in the marginal zone of the spleen. *Nat. Immunol.* 2011;13(2):170–180.

600 52. Coquery CM et al. Neutrophils contribute to excess serum BAFF levels and promote CD4+ T cell
601 and B cell responses in lupus-prone mice. *PloS One* 2014;9(7):e102284.

602 53. Parsa R et al. BAFF-secreting neutrophils drive plasma cell responses during emergency
603 granulopoiesis. *J. Exp. Med.* 2016;213(8):1537–1553.

604 54. Chorny A et al. The soluble pattern recognition receptor PTX3 links humoral innate and adaptive
605 immune responses by helping marginal zone B cells. *J. Exp. Med.* 2016;213(10):2167–2185.

606 55. Cerutti A, Puga I, Magri G. The B cell helper side of neutrophils. *J. Leukoc. Biol.* 2013;94(4):677–
607 682.

608 56. Dosenovic P et al. BLyS-mediated modulation of naive B cell subsets impacts HIV Env-induced
609 antibody responses. *J. Immunol.* 2012;188(12):6018–6026.

610 57. Enoksson SL et al. The inflammatory cytokine IL-18 induces self-reactive innate antibody
611 responses regulated by natural killer T cells. *Proc. Natl. Acad. Sci. U. S. A.* 2011;108(51):E1399-1407.

612 58. Lopes-Carvalho T, Foote J, Kearney JF. Marginal zone B cells in lymphocyte activation and
613 regulation. *Curr. Opin. Immunol.* 2005;17(3):244–250.

614 59. McCulloch L, Smith CJ, McColl BW. Adrenergic-mediated loss of splenic marginal zone B cells
615 contributes to infection susceptibility after stroke. *Nat. Commun.* 2017;8:15051.

616 60. Srivastava B, Quinn WJ, Hazard K, Erikson J, Allman D. Characterization of marginal zone B cell
617 precursors. *J. Exp. Med.* 2005;202(9):1225–1234.

618 61. Schweighoffer E et al. The BAFF receptor transduces survival signals by co-opting the B cell
619 receptor signaling pathway. *Immunity* 2013;38(3):475–488.

620 62. Scapini P et al. Proinflammatory mediators elicit secretion of the intracellular B-lymphocyte
621 stimulator pool (BLyS) that is stored in activated neutrophils: implications for inflammatory diseases.
622 *Blood* 2005;105(2):830–837.

623 63. Matsumoto M, Fu YX, Molina H, Chaplin DD. Lymphotoxin-alpha-deficient and TNF receptor-I-
624 deficient mice define developmental and functional characteristics of germinal centers. *Immunol. Rev.*
625 1997;156:137–144.

626 64. Banks TA et al. Lymphotoxin-alpha-deficient mice. Effects on secondary lymphoid organ
627 development and humoral immune responsiveness. *J. Immunol.* 1995;155(4):1685–1693.

628 65. Fu YX et al. Lymphotoxin-alpha (LTalpha) supports development of splenic follicular structure
629 that is required for IgG responses. *J. Exp. Med.* 1997;185(12):2111–2120.

630 66. Fu YX, Huang G, Wang Y, Chaplin DD. Lymphotoxin-alpha-dependent spleen microenvironment
631 supports the generation of memory B cells and is required for their subsequent antigen-induced
632 activation. *J. Immunol.* 2000;164(5):2508–2514.

633 67. Jackson SW et al. B cell IFN-γ receptor signaling promotes autoimmune germinal centers via cell-
634 intrinsic induction of BCL-6. *J. Exp. Med.* 2016;213(5):733–750.

635 68. Casulli S, Elbim C. Interactions between human immunodeficiency virus type 1 and
636 polymorphonuclear neutrophils. *J. Innate Immun.* 2014;6(1):13–20.

637 69. Shi X et al. Neutropenia during HIV infection: adverse consequences and remedies. *Int. Rev.*
638 *Immunol.* 2014;33(6):511–536.

639 70. Li L et al. Am80-GCSF synergizes myeloid expansion and differentiation to generate functional
640 neutrophils that reduce neutropenia-associated infection and mortality. *EMBO Mol. Med.*
641 2016;8(11):1340–1359.

642 71. Scapini P et al. G-CSF-stimulated neutrophils are a prominent source of functional BLyS. *J. Exp.*
643 *Med.* 2003;197(3):297–302.

644 72. Bowers NL et al. Immune suppression by neutrophils in HIV-1 infection: role of PD-L1/PD-1
645 pathway. *PLoS Pathog.* 2014;10(3):e1003993.

646 73. Sips M et al. Fc receptor-mediated phagocytosis in tissues as a potent mechanism for preventive

and therapeutic HIV vaccine strategies. *Mucosal Immunol.* 2016;9(6):1584–1595.

74. Albanesi M et al. Neutrophils mediate antibody-induced antitumor effects in mice. *Blood* 2013;122(18):3160–3164.

75. Cittera E et al. The CCL3 family of chemokines and innate immunity cooperate in vivo in the eradication of an established lymphoma xenograft by rituximab. *J. Immunol.* 2007;178(10):6616–6623.

76. Golay J et al. Glycoengineered CD20 antibody obinutuzumab activates neutrophils and mediates phagocytosis through CD16B more efficiently than rituximab. *Blood* 2013;122(20):3482–3491.

77. Hernandez-Ilizaliturri FJ et al. Neutrophils contribute to the biological antitumor activity of rituximab in a non-Hodgkin's lymphoma severe combined immunodeficiency mouse model. *Clin. Cancer Res.* 2003;9(16 Pt 1):5866–5873.

78. Valgardsdottir R et al. Human neutrophils mediate trogocytosis rather than phagocytosis of CLL B cells opsonized with anti-CD20 antibodies. *Blood* 2017;129(19):2636–2644.

79. Guyre CA, Gomes D, Smith KA, Kaplan JM, Perricone MA. Development of an in vivo antibody-mediated killing (IVAK) model, a flow cytometric method to rapidly evaluate therapeutic antibodies. *J. Immunol. Methods* 2008;333(1–2):51–60.

80. Chen W, Qin H, Chesebro B, Cheever MA. Identification of a gag-encoded cytotoxic T-lymphocyte epitope from FBL-3 leukemia shared by Friend, Moloney, and Rauscher murine leukemia virus-induced tumors. *J. Virol.* 1996;70(11):7773–7782.

81. Peranzoni E et al. Ex Vivo Imaging of Resident CD8 T Lymphocytes in Human Lung Tumor Slices Using Confocal Microscopy. *J. Vis. Exp. JoVE* [published online ahead of print: December 27, 2017];(130). doi:10.3791/55709

FIGURES

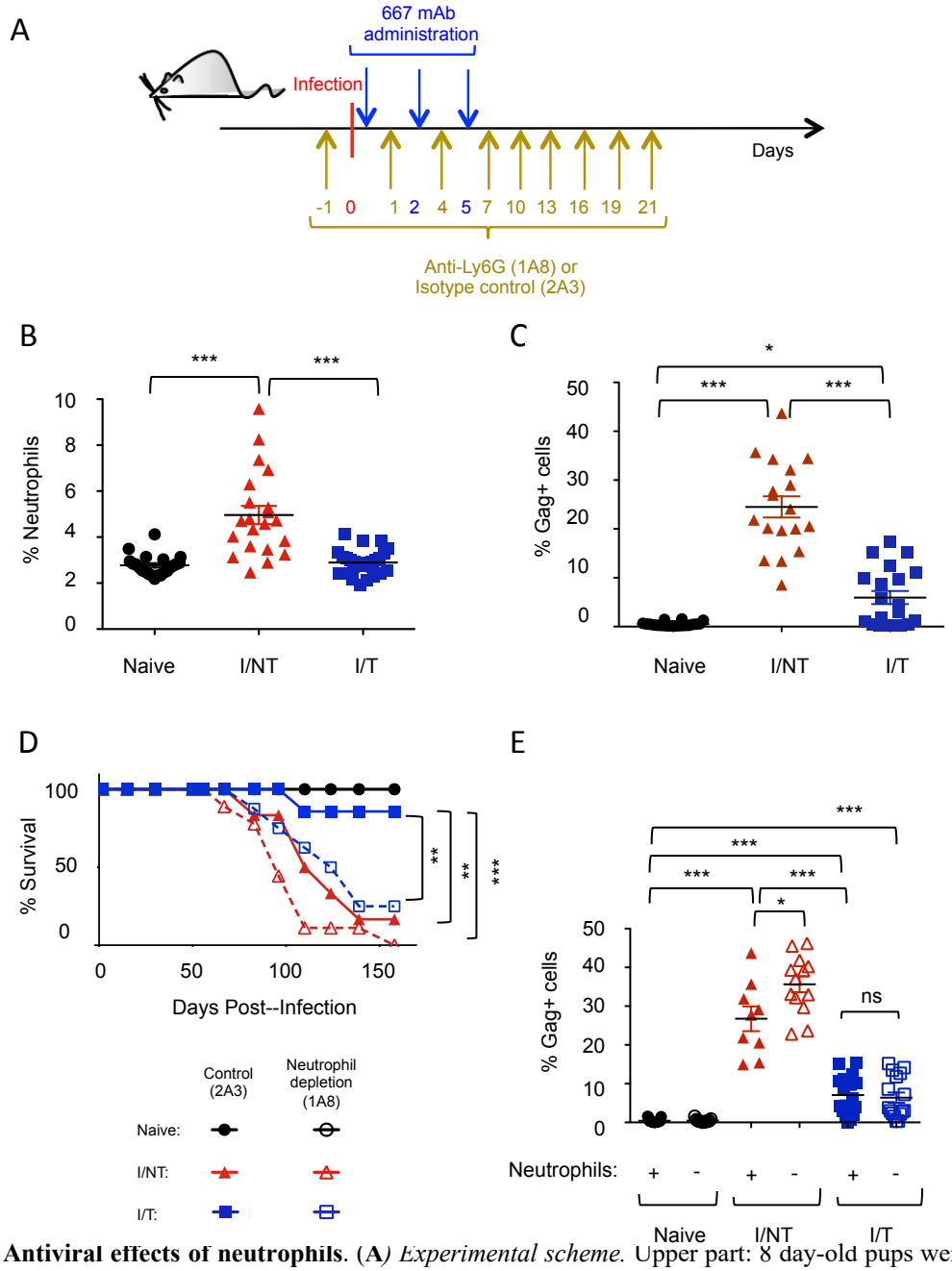

Figure 1. Antiviral effects of neutrophils. (**A**) *Experimental scheme.* Upper part: 8 day-old pups were infected and treated with the 667 mAb as indicated. Lower part: mice were treated as indicated with the anti-Ly6G 1A8 mAb or the isotype control 2A3 mAb in neutrophil depletion experiments. (**B-C**) *Neutrophil recruitment and infected cells rate in spleen.* Splenocytes from naive, infected/non-treated (I/NT) and infected/treated (I/T) mice were analyzed by flow cytometry on day 8 p.i. for (i) neutrophil recruitment (% of $Ly6G^+$ cells) and (ii) for retroviral positivity of splenocytes (% of Gag^+ cells) gated in the $CD45.2^+$ population. The data presented correspond to 5 independent experiments with at least 15 mice per group. (**D**) *Mouse survival*. Naive, I/NT and I/T mice were treated with either the anti-neutrophil- (1A8) or the control (2A3) mAb as indicated in (**A**) and followed up for leukemic death. The data represent 2 independent experiments with 6-9 mice per group. (**E**) *Infected cells rate upon neutrophil depletion*. Neutrophils of naive, I/NT and I/T mice were depleted, or not, as indicated in (**A**) and infected splenocytes were assayed as in (**C**) on day 8 p.i. The data represent 4 independent experiments with 9-15 mice per group. Data are expressed as means +/- SEM. Statistical significance was established using a parametric one-way ANOVA test with a Bonferroni correction. (*$p < 0.05$; **$p < 0.01$; ***$p < 0.001$).

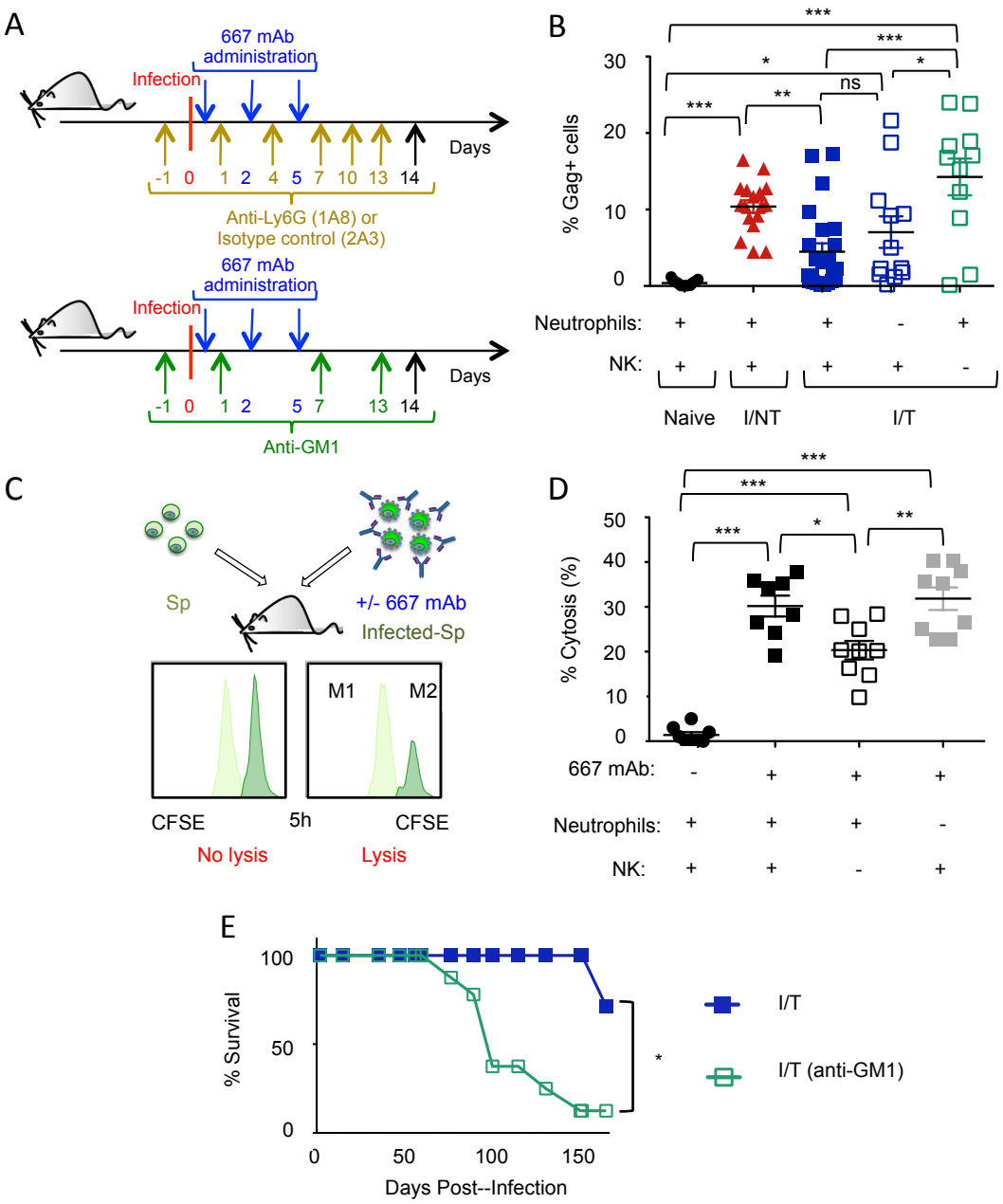

Figure 2. Antibody-mediated control of viral propagation by NKs. (**A**) *Experimental scheme*. Mice were infected and mAb-treated as in Fig 1A. Upper part: infected/treated mice were treated as indicated with the anti-Ly6G 1A8 mAb or the isotype control 2A3 mAb to deplete neutrophils. Lower part: infected/treated mice were treated as indicated with the anti-asialo-GM1 antibody to deplete NKs. (**B**) *Effect of neutrophils or NKs depletion in viral spread in infected/treated mice.* Percentage of infected cells at day 14 p.i in the spleen of naive-, I/NT- and I/T mice, depleted or not in neutrophils or NKs assessed as in Fig 1C. The data represent 3 independent experiments with at least 8 mice per group.Data are expressed as means +/- SEM. (*p<0,05, **p < 0.01,***p<0,001). (**C-D**) *In vivo* cytolysis activity of 667 in naive mice after depletion of neutrophils or NKs. Splenocytes from non-infected mice (Sp) were labelled using 0.5 µM of the vital dye CFSE ($CFSE^{low}$ cells; M1) and mixed at a 1:1 ratio with splenocytes from infected mice (Infected-Sp) labelled using 5 µM CFSE ($CFSE^{high}$ cells; M2) and pre-incubated, or not, with the 667 mAb. Mixed cell populations were administered to naive mice 1 day after depletion of either neutrophils or NKs with the 1A8 mAb or the anti-asialo-GM1 antibody, respectively. Cytolysis was quantified 5 hours later as described in Methods section. The data are presented as mean ± SEM of 2 independent experiments with at least 8 mice per group. Statistical significance was established using a parametric one-way ANOVA test with a Bonferroni correction (panels B and D). (**E**) *Effect of NKs depletion in the survival of infected/treated mice.* I/T, NKs-depleted or not as indicated in (**A**) were followed up for leukemic death. The data represent 2 independent experiments with 7 mice per group. Statistical significance was established using an unpaired Student's test.

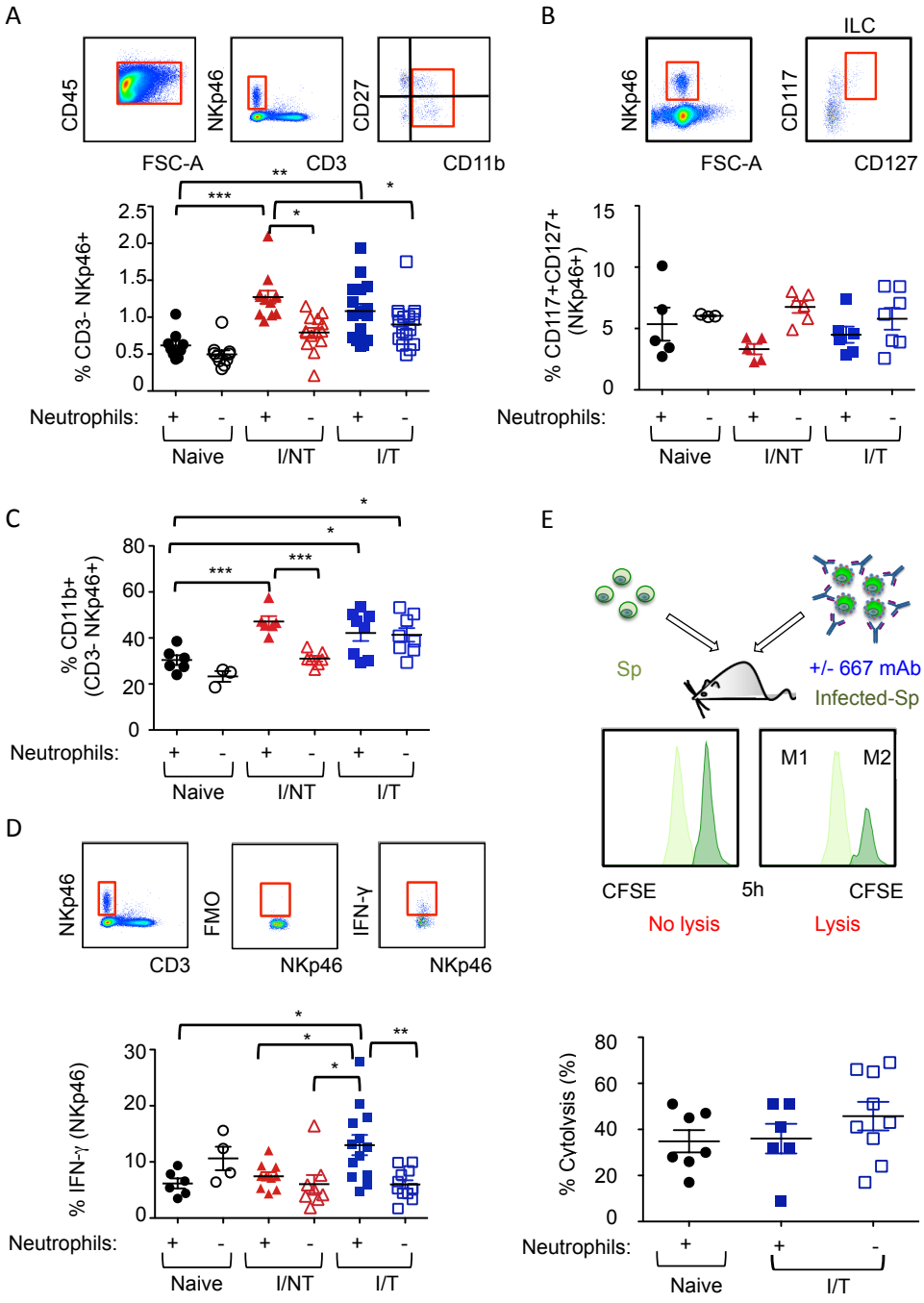

Figure 3. Effects of neutrophil depletion on innate lymphoid cells recruitment and biology. (**A-D**) Neutrophils of naive, I/NT and I/T mice were depleted, or not, as indicated in Figure 1A and ILC in the spleen were assayed 14 days p.i. by flow cytometry. (**A**) *Frequency of CD3$^-$NKp46$^+$ cells* in the CD45.2$^+$ leukocytic population. (**B**) *Frequency of CD117$^+$/CD127$^+$ cells in the Lin$^-$NKp46$^+$ population*. (**C**) *Maturation* (CD11b$^+$ cells) and (**D**) *expression of IFN-γ in the CD3$^-$NKp46$^+$ population*. (**E**) *In vivo cytolysis activity of 667 in infected/treated mice after depletion of neutrophils*. The 1A8, or the 2A3 isotype control mAb, were administered to I/T mice and 667 ADCC activity was quantified at 30 days p.i. as in Fig 2C-2D. The data represent at least 2 independent experiments. Data are expressed as means +/- SEM. Statistical significance was established using a parametric one-way ANOVA test with a Bonferroni correction (*p < 0.05; **p < 0.01; ***p < 0.001).

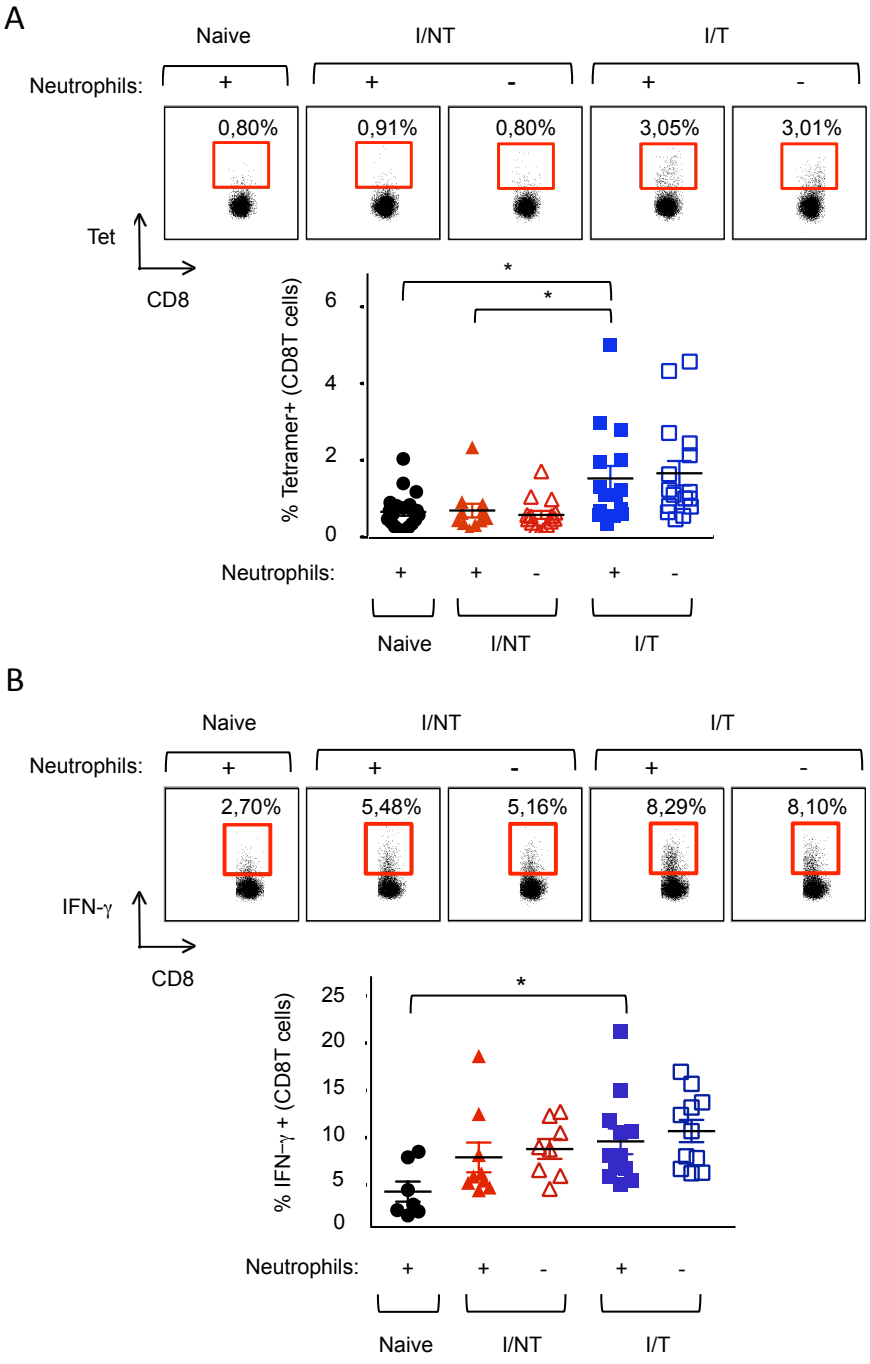

Figure 4. Assay of FrCasE-specific CD8$^+$ T cells in the presence and absence of neutrophils. Neutrophils of naive, I/NT and I/T mice were depleted, or not, as indicated in (**A**). *Frequency of FrCasE-specific CD8$^+$ T cells.* Spleen cells were isolated at day 14 p.i. and the frequency of virus-specific CD8$^+$ T cells in the total CD8$^+$ T-cells population was assayed by flow cytometry using the H2D^b-GagL MHC tetramer. The data represent 4 independent experiments with at least 11 mice per group. (**B**) *Expression of IFN-γ by CD8$^+$ T cells*. Splenic CD8$^+$ T cells were flow cytometry-analyzed for the expression of IFN-γ. The data presented represent 3 independent experiments with at least 7 mice per group. Data are expressed as means +/- SEM. Statistical significance was established using a parametric one-way ANOVA test with a Bonferroni correction (*p< 0,05).

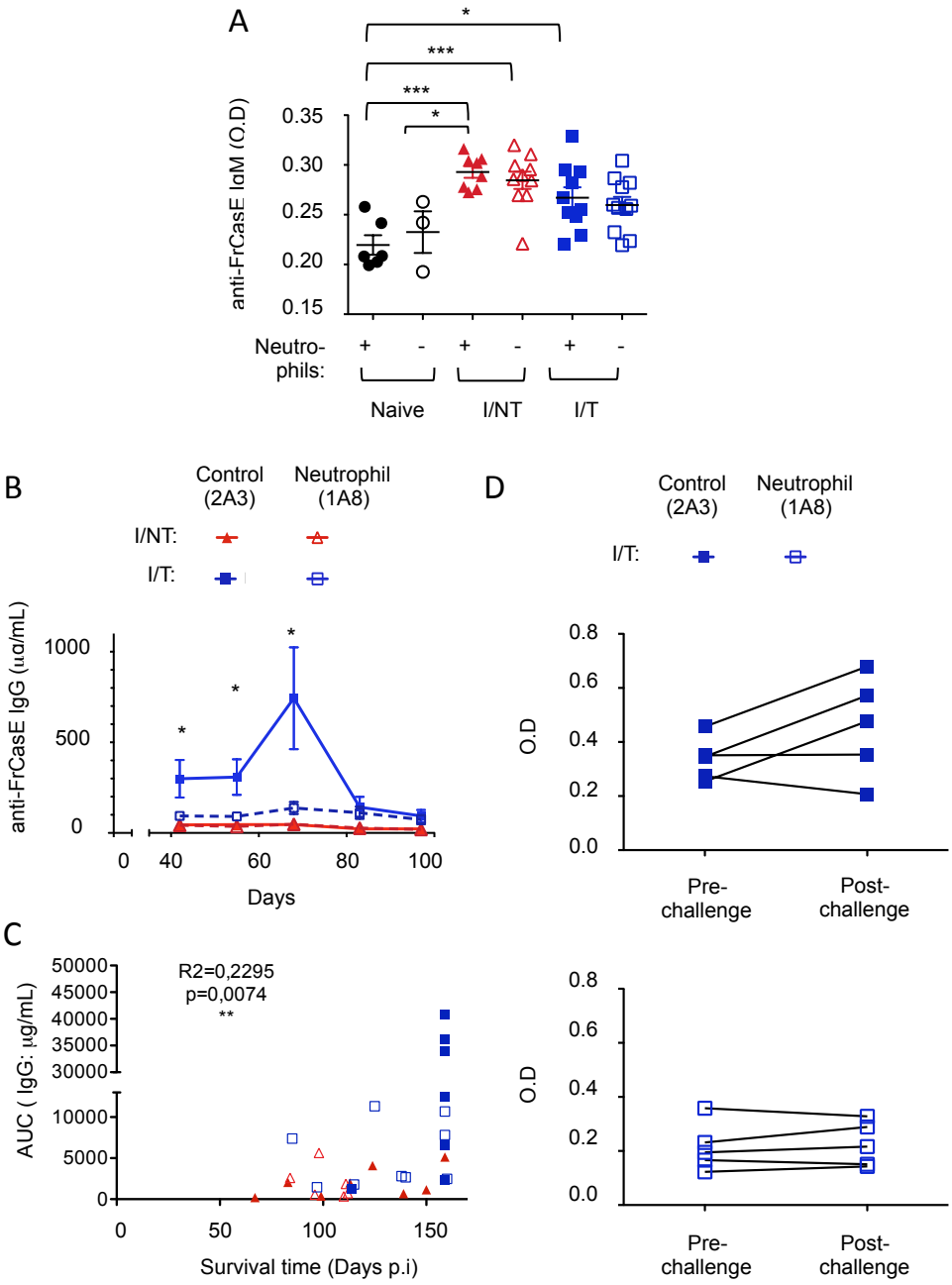

Figure 5. Enhancement of the humoral antiviral response by neutrophils. Neutrophils of naive, I/NT and I/T mice were depleted, or not, as indicated in Figure 1A. (**A, B)** *Serum concentration of FrCasE-specific Igs.* (**A)** Seric FrCasE-specific IgM levels were assayed by ELISA at 14 days p.i. The data represent 2 independent experiments with 8-11 mice per group (for I/NT and I/T mice) and 3 to 6 mice per group (for naive mice). (**B)** Seric FrCasE-specific IgG concentration was assayed by ELISA at the indicated times. The data represent 2 independent experiments with 7-9 mice per group. Data are expressed as means +/- SEM. Statistical significance was established using a parametric one-way ANOVA test with a Bonferroni correction (*$p < 0.05$; **$p < 0.01$; ***$p < 0.001$). (**C**) *Correlation between serum anti-FrCasE IgG levels* (evaluated as the area under the curve; AUC) *and survival times*, analyzed using the Pearson correlation test. AUC was evaluated until the last time point at which all mice were still alive (day 68 p.i). All infected/non-treated- (n = 8), infected/treated- (n = 9) mice, depleted or not in neutrophils (n = 9 and n = 7, respectively), showed in Fig 1D were evaluated for such a correlation. (**D**) *FrCasE-specific secondary humoral response.* Seric FrCasE-specific IgG levels in I/T mice (depleted or not in neutrophils) were assayed by ELISA before and 1 week after a viral challenge performed at day 93 p.i. The data represent 2 independent experiments with 5 mice per group. Statistical significance was established using a paired Student's t test.

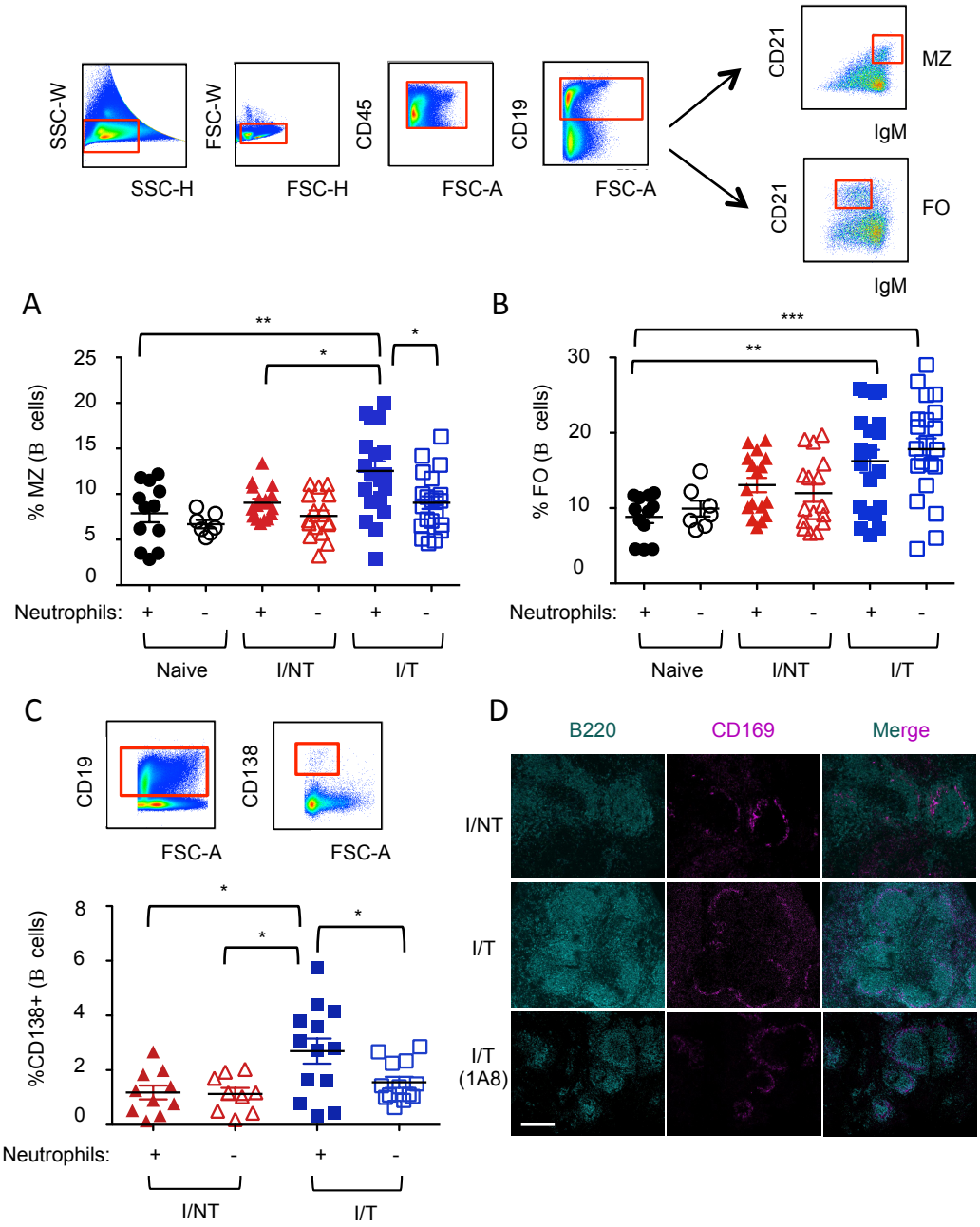

Figure 6. Effects of neutrophil depletion on B-cell responses. (**A-D**) Neutrophils of naive, I/NT and I/T mice were depleted, or not, as indicated in Figure 1A. (**A-B**) *Frequency of MZ and follicular (FO) B cells*. Spleen cells were isolated at day 14 p.i. and flow cytometry-analyzed for the frequency of MZ ($CD21^{high}IgM^{high}$) (**A**) and FO ($CD23^{+}IgM^{low}$) (**B**) $CD19^{+}$ B cells. (**C**) *Frequency of plasma cells.* BM cells were isolated at day 14 p.i. and flow cytometry-analyzed for the frequency of $CD138^{+}$ ($CD19^{+}$) B cells. The data represent 5 independent experiments with 7-12 mice per group for naive mice and 17-21 per group for I/NT and I/T mice. Data are expressed as means +/- SEM. Statistical significance was established using a parametric one-way ANOVA test with a Bonferroni correction. (*$p < 0.05$; **$p < 0.01$; ***$p < 0.001$). (**D**) *Histological analyses of spleen sections.* Immunolabelling of B cells ($B220^{+}$) and macrophages of the MZ ($CD169^{+}$) was performed in sections from spleens of infected/non-treated and infected/treated mice (depleted or not in neutrophils) recovered at 14 days p.i. to visualize germinal centers. The images are representative of four separate mice for each experimental condition. Scale bar 200 µm.

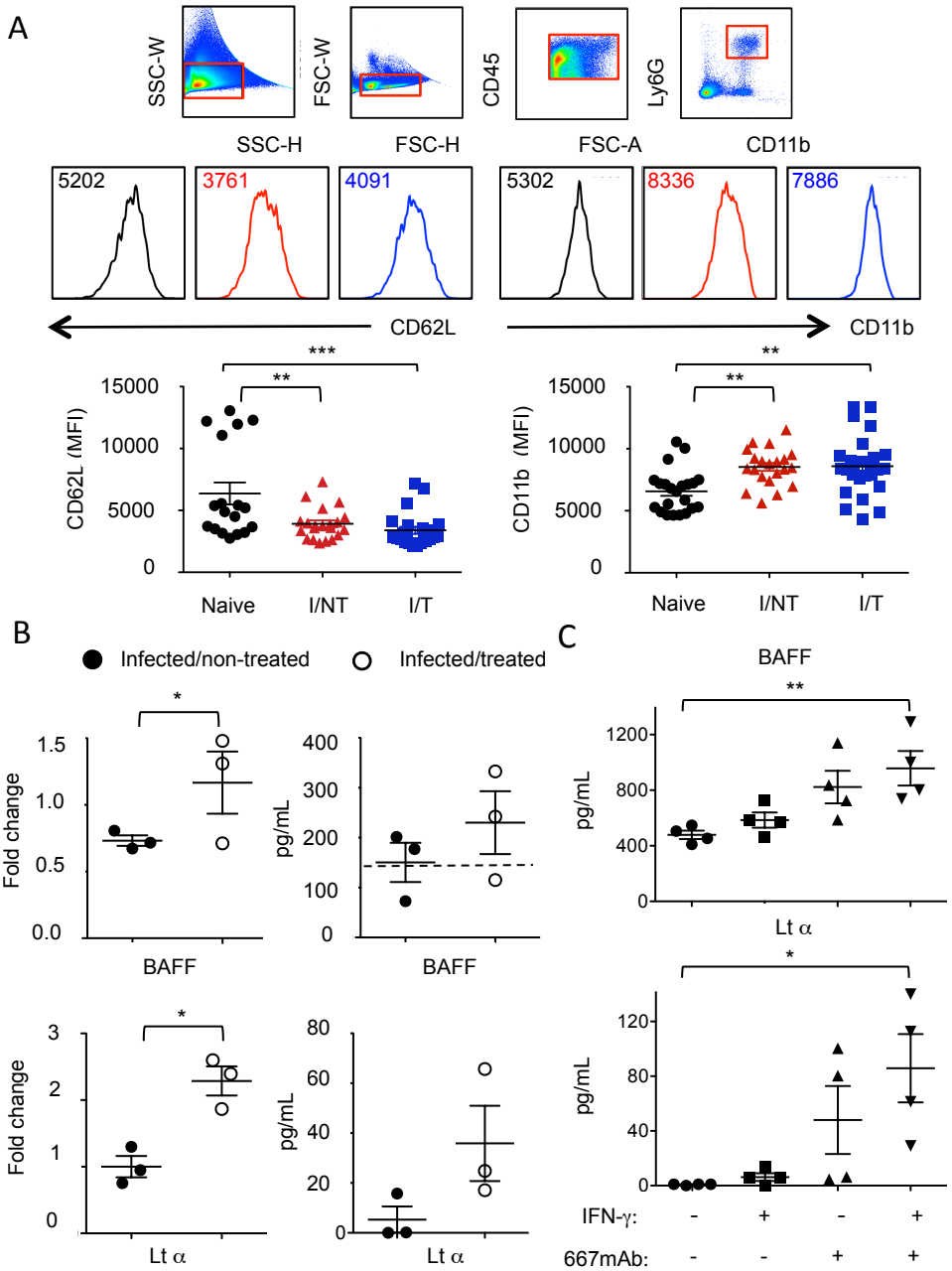

Figure 7. Activation of splenic and BM-isolated neutrophils. (**A**) *Expression of CD11b and CD62L*. Spleen cells from naive, I/NT and I/T mice were isolated at day 8 p.i. and flow cytometry-analyzed for assaying cell surface expression of CD11b and CD62L. The data represent 5 independent experiments with at least 18 mice per group. Data are expressed as means +/- SEM. (**B**) *Expression and protein release of BAFF and LTα by neutrophils.* Neutrophils from naive, I/NT and I/T mice were sorted from the spleen at day 8 p.i. and assessed for cytokine expression or protein release. Cytokine expression (left) was assessed by RT-qPCR normalized to β-actin. The data show fold changes in cytokine expression by neutrophils from I/NT and I/T mice as compared to naive mice and are representative of 3 independent experiments with 8-10 mice per group. Protein release (right) was assessed by ELISA in supernatants of sorted neutrophils cultured at a density of 10^5 cells/well for 24 h. The data show BAFF and LTα release by neutrophils from I/NT and I/T and are representative of 3 independent experiments with 8-10 mice per group. The dashed line represents the level of BAFF released by neutrophils sorted from naive mice. No LTα release was detected from neutrophils sorted from naive mice. . (**C**) *BAFF and LTα release by BM-isolated neutrophils.* BAFF and LTα release was assessed by ELISA in supernatants of neutrophils isolated from BM of naive mice (>95% purity) and cultured for 24 h in 667-mAb coated 24-well plates at a density of 2×10^6 cells in 500 µl of medium. Experiments were done in the presence and in the absence of the pro-inflammatory cytokine IFN-γ (100 μg/ml). 667 mAb non-coated plates were used as control. The data represent 4 independent experiments. Data are expressed as means +/- SEM. Statistical significance was established using a parametric one-way ANOVA test with a Bonferroni correction (panels A and C) or a paired Student's t test (panel B). (*$p < 0.05$; **$p < 0.01$; ***$p < 0.001$).